



This is a repository copy of *How do toxicants affect epidemiological dynamics?*.

White Rose Research Online URL for this paper:
<http://eprints.whiterose.ac.uk/140412/>

Version: Accepted Version

Article:

Booton, R.D., Iwasa, Y. and Childs, D.Z. orcid.org/0000-0002-0675-4933 (2018) How do toxicants affect epidemiological dynamics? *Oikos*. ISSN 0030-1299

<https://doi.org/10.1111/oik.05654>

This is the peer reviewed version of the following article: Booton, R. D., Iwasa, Y. and Childs, D. Z. (2018), How do toxicants affect epidemiological dynamics?. *Oikos*, which has been published in final form at <https://doi.org/10.1111/oik.05654>. This article may be used for non-commercial purposes in accordance with Wiley Terms and Conditions for Self-Archiving.

Reuse

Items deposited in White Rose Research Online are protected by copyright, with all rights reserved unless indicated otherwise. They may be downloaded and/or printed for private study, or other acts as permitted by national copyright laws. The publisher or other rights holders may allow further reproduction and re-use of the full text version. This is indicated by the licence information on the White Rose Research Online record for the item.

Takedown

If you consider content in White Rose Research Online to be in breach of UK law, please notify us by emailing eprints@whiterose.ac.uk including the URL of the record and the reason for the withdrawal request.



eprints@whiterose.ac.uk
<https://eprints.whiterose.ac.uk/>

1 Running title: How do toxicants affect epidemiological dynamics?

2

3 **How do toxicants affect epidemiological** 4 **dynamics?**

5

6 **Ross D. Booton^{1,*}, Yoh Iwasa² & Dylan Z. Childs¹**

7

8 1 Department of Animal and Plant Sciences, University of Sheffield, Sheffield, United
9 Kingdom

10 2 Department of Bioscience, School of Science and Technology, Kwansei-Gakuin
11 University, Japan

12 * Corresponding author. rbooton@gmail.com

13 ORCID ID: ORCID ID: 0000-0002-3013-4179

14

15 **Abstract**

16

17 Populations are formed of their constituent interacting individuals, each with their own
18 respective within-host biological processes. Infection not only spreads within the host
19 organism but also spreads between individuals. Here we propose and study a
20 multilevel model which links the within-host statuses of immunity and parasite density
21 to population epidemiology under sublethal and lethal toxicant exposure. We analyse
22 this nested model in order to better understand how toxicants impact the spread of
23 disease within populations. We demonstrate that outbreak of infection within a
24 population is completely determined by the level of toxicant exposure, and that it is
25 maximised by intermediate toxicant dosage. We classify the population epidemiology
26 into 5 phases of increasing toxicant exposure and calculate the conditions under which
27 disease will spread, showing that there exists a threshold toxicant level under which
28 epidemics will not occur. In general, higher toxicant load results in either extinction of
29 the population or outbreak of infection. The within-host statuses of the individual host
30 also determine the outcome of the epidemic at the population level. We discuss
31 applications of our model in the context of environmental epidemiology, predicting that
32 increased exposure to toxicants could result in greater risk of epidemics within
33 ecological systems. We predict that reducing sublethal toxicant exposure below our
34 predicted safe threshold could contribute to controlling population level disease and
35 infection.

36

37 **Keywords:** epidemiology; host-parasite interactions; immunity; nested model;
38 population dynamics; toxicant stress

39 Introduction

40 The spread of infectious disease within populations occurs at various scales of
41 organisation. Population-scale processes are determined by the interacting individuals
42 within such populations, each with their own respective individual within-host biological
43 processes. Between-host epidemiological dynamics are determined primarily by host
44 demography and transmission (Grenfell and Harwood 1997), while transmission is
45 determined by the level of disease in infected individuals within the population (Mideo
46 et al. 2008). Furthermore, the dynamics of diseased individuals are entirely dependent
47 on their corresponding within-host parasite load and host defence mechanisms (Mideo
48 et al. 2008). Infectious diseases such as host-parasite interactions depend upon two
49 processes; both the immunological host-parasite interaction and the subsequent
50 population level epidemiology (Feng et al. 2012).

51

52 Individual organisms are exposed to a wide variety of stressors. These stressors can
53 be broadly defined as either abiotic (anthropogenic or climatic) or biotic (parasites or
54 predation). These stressors either act alone, or in combination which can result in a
55 higher than expected overall effect when synergistic interactions occur between them
56 (Holmstrup et al. 2010). One such anthropogenic stressor is toxicant exposure;
57 chemicals released into the environment which damage or have other detrimental
58 effects on the host. Examples of such chemical stressors include pesticides in
59 freshwater systems (Relyea and Hoverman 2006), neonicotinoid insecticides in honey
60 bee colonies (Goulson et al. 2015), various environmental pollutants in rotifers (Snell
61 and Janssen 1995) and *Daphnia* (Buratini et al. 2004) and polychlorinated dibenzo-p-
62 dioxins (PCDDs), biphenyls (PCBs) and dibenzofurans (PCDFs) in animals and
63 humans (Van Den Berg et al. 1998). Indeed, toxicants affect a wide range of non-

64 target species, including birds, mammals (Eason et al. 2002), aquatic species (Phipps
65 and Holcombe 1985), and insects (Pisa et al. 2015).

66

67 In general, toxicants have lethal effects (Martin and Holdich 1986, Suchail et al. 2001,
68 Iwasa et al. 2004, Blacquièrè et al. 2012, Pan et al. 2014, Wang et al. 2017), where
69 the direct chronic lethality of toxicant exposure occurs at high doses (Suchail et al.
70 2001, Pan et al. 2014, Wang et al. 2017). Toxicants often have other effects on
71 behaviour, learning, feeding, memory and fecundity (Warner et al. 1966, Davies et al.
72 1994, Decourtye et al. 2003, Han et al. 2010, Williamson and Wright 2013, Williams
73 et al. 2015). Individuals exposed to toxicants can face other stressors such as parasite
74 infections which, when combined can cause further damage to the host. For example,
75 the combination of parasite infection and toxicant exposure can increase the initial
76 parasite load (Pettis et al. 2012, Doublet et al. 2015), increase virulence (Coors et al.
77 2008) and increase mortality (Alaux et al. 2010, Vidau et al. 2011) in the host. These
78 interactions between toxicants and parasites are observed in a multitude of organisms
79 (Holmstrup et al. 2010). In addition to the effects of toxicants on the functionality of the
80 host, toxicants also sublethally damage or inhibit the individual immune response of
81 the host (James and Xu 2012). There are a wide range of immunosuppressive effects
82 which occur as a result of sublethal or field realistic levels of toxicant exposure (Bols
83 et al. 2001, Gilbertson et al. 2003, James and Xu 2012, Mason 2013, Brandt et al.
84 2016). Throughout this manuscript we will focus on these two simultaneous effects of
85 toxicant damage to the host, and refer to them as follows: lethal exposure reduces the
86 functionality of the host, while sublethal exposure causes a reduction in the
87 functionality of the host immune response.

88

89 The individual impacts of stressors on host level processes are well studied, but the
90 subsequent impact on higher scales of organisation such as populations are often not
91 fully understood (Kohler and Triebkorn 2013). Toxicant research tends to focus either
92 on the molecular, physiological or cellular levels, or on merely observing population
93 decline, with the causal link between scales (within-host and population) rarely
94 investigated (Kohler and Triebkorn 2013). For example, lethal and sublethal
95 thresholds of toxicants are determined through experiments with individuals, leading
96 to uncertainty as to what consequence this has for the population level (Gergs et al.
97 2013). Furthermore, interactions between multiple stressors lead to effects which are
98 not predictable from understanding the individual effects of each stressor (Coors et al.
99 2008). For example, the chemical stressor cadmium, in combination with other abiotic
100 stressors can affect the population growth rate and life-history parameters of *Daphnia*
101 *magna* (Heugens et al. 2006). Uncertainty in quantifying toxic effects can be explained
102 through their interaction with other stressors at the individual level, which in turn alter
103 the population dynamics (Heugens et al. 2006). In another study with *Daphnia magna*,
104 pesticide exposure has been shown to enhance the virulence of endoparasites (Coors
105 et al. 2008).

106

107 Many mathematical models either consider the within-host dynamics independent of
108 the population (Booton et al. 2018), the epidemiological population dynamics
109 independent of the within-host parasite dynamics (Anderson and May 1992, Nowak
110 and May 2000), or model stressors as general population level processes (Bryden et
111 al. 2013, Booton et al. 2017, Henry et al. 2012). Bridging multi-scale biological
112 processes can be achieved using nested (also called embedded) mathematical
113 models (Gilchrist and Sasaki 2002, Mideo et al. 2008). Nested approaches embed

114 models of within-host dynamics into the epidemiological population scale. This allows
115 epidemiological parameters such as the basic reproduction number R_0 to be
116 determined by the dynamics of within-host parameters such as parasite load, immune
117 status and cellular health. This approach is particularly useful when the effects of
118 within-host processes on determining population epidemiology are unknown (Mideo
119 et al. 2008), and as such, parameter relationships can be determined from the
120 subsequent analysis of the nested model, providing important biological mechanistic
121 predictions (Gilchrist and Sasaki 2002, Alizon and van Baalen 2005, Gilchrist and
122 Coombs 2006, Feng et al. 2012; 2013; 2015). For example, the model by Bhattacharya
123 and Martcheva (2016) relates the immune response of a species infected by a
124 pathogen to population epidemiological parameters, using a nested within- and
125 between-host approach. This study however focusses on ecological competition
126 between species, rather than additional sources of stressors such as toxicants.

127

128 To date, little work addresses the interface between population epidemiology and
129 toxicant stress (Lundin et al. 2015, Bhattacharya and Martcheva 2016). In this study,
130 we examine how toxicants impact the spread of disease within populations, and how
131 the subsequent epidemiology is formed from their respective within- and between-host
132 processes. We introduce and analyse a nested model linking epidemiological
133 between-host processes to those of a previously studied within-host model (Booton et
134 al. 2018). This previous model examined interacting within-host processes: host
135 immunity, host parasite load and host cellular health, and the effects of sublethal and
136 lethal toxicant exposure. This previous study by Booton et al. (2018) showed that
137 within-host parasite density is maximised by intermediate doses of toxicant exposure,
138 but they did not consider the subsequent effects of their results on population level

139 epidemiology. Here, we investigate the change in the basic reproduction number of
140 the epidemic as the toxicant load is increased from zero to extremely high exposure
141 (causing host mortality) and classify the resulting epidemiology into five distinct
142 phases of infection. These phases are determined by the interplay between both
143 within-host and between-host dynamics and processes.

144

145 **Methods**

146 Here we consider two scales of biological organisation, both the within-host immuno-
147 infection dynamics and between-host population dynamics. We assume that the
148 within-host dynamics are fast relative to a slower population level timescale, a
149 commonly used method for linking multi-level scales ([Gilchrist and Coombs 2006](#),
150 [Mideo et al. 2008](#), [Feng et al. 2013](#)). Therefore, each individual has equal average
151 status of infection at the within-host level, dependent upon the individual's sub-class
152 of infection (susceptible or infected). This significantly reduces the complexity of such
153 nested models, and allows a substitution of within-host steady state values into the
154 between-host system. The separation of time scales through slow-fast dynamics is
155 justified through assuming that each individual belongs to a sub-group of infection,
156 which we characterise below as either susceptible or infected.

157

158 **Within-host model**

159 We use the simple modelling framework provided in [Booton et al. \(2018\)](#) to describe
160 the within-host infection dynamics under toxicant exposure in an individual. X , Y and
161 Z represent the uninfected within-host cells, parasite density and immune function,
162 respectively. The within-host cells X represent the total number of uninfected cells

163 within the host and Y represents the total number of parasite-infected cells as a
164 measure of parasite density. Here the term uninfected implies that these cells could
165 be potentially infected by a parasite. To simplify the analysis significantly we use a
166 non-dimensionalised version of the original model published in [Booton et al. \(2018\)](#).
167 The full derivation of this model can be found in the electronic supplement, and this
168 model has the same qualitative dynamics, but with fewer parameters.

169

$$170 \quad \frac{dX}{dt} = (1 - \xi_1 Q) - X(\phi + Y) \quad (1a)$$

$$171 \quad \frac{dY}{dt} = Y(\epsilon X - \gamma - \omega Z) \quad (1b)$$

$$172 \quad \frac{dZ}{dt} = (1 - \xi_2 Q) - Z \quad (1c)$$

173 Toxicant exposure Q both reduces the functionality of the immune system at rate ξ_2
174 (sublethal) relative to the production of immunity and damages the functionality of the
175 host at rate ξ_1 (lethal) relative to the production of new cells. This relationship is the
176 simplest possible assumption regarding the effects of the toxicant on the host, and
177 other such assumptions (such as density-dependence) reproduce qualitatively
178 equivalent results to the model presented here ([Booton et al. 2018](#)). Therefore, we
179 assume a constant rate of sublethal and lethal effects on the host, as this the simplest
180 way of reproducing within-host toxicant dynamics. Within the model for any given level
181 of exposure we will consider the simultaneous lethal (i.e. on host function) and
182 sublethal (i.e. on host immunity) effects of the toxicant. The non-dimensionalisation
183 process scaled the remaining parameters relative to the removal of immunity: ϕ sets
184 the rate at which healthy cells are removed from the system, ϵ represents transmission
185 of parasites and production of cells, γ sets the death rate of the parasites, and ω
186 represents the immune suppression and production of immunity (all relative to the

187 removal of immunity). Details on within-host parameter relationships and their
188 substitutions can be found in the electronic supplement.

189

190 This model assumes to begin with that $1 - \xi_1 Q > 0$ and $1 - \xi_2 Q > 0$. At the point when
191 $Z = 0$, equation (1c) is removed and the model becomes the system of equations (1a)
192 and (1b) without the term $-\omega YZ$ (as $Z = 0$). In general, throughout this paper we
193 assume $\xi_2 > \xi_1$, which ensures sensible behaviour of the model. If the alternative
194 assumption $\xi_2 < \xi_1$ holds true, the model predicts a healthy immune function even
195 after the parasite and healthy cells are dead (representing host mortality). The effects
196 of this alternative assumption can be found in the electronic supplement. However we
197 focus on the case $\xi_2 > \xi_1$ and argue that this case is biologically valid since the direct
198 lethality of toxicants generally occur at higher doses (Suchail et al. 2001, Pan et al.
199 2014, Wang et al. 2017), and various types of immunosuppressive damage occur at
200 sublethal or field realistic levels of toxicant (Bols et al. 2001, James and Xu 2012,
201 Brandt et al. 2016). Hence the assumption $\xi_2 > \xi_1$ ensures that the relative effect of
202 sublethal damage is stronger than that of the lethal toxicant damage at lower doses.
203 Similarly, after $Y = 0$, the model becomes equation (1a) but without the term $-XY$. The
204 assumption that $Z = 0$ before $Y = 0$ ensures that we can investigate both the sublethal
205 immunosuppressive effect and direct lethality (reducing host function) of the toxicant
206 before the death of the host at higher levels of Q .

207

208 We define X' to be the equilibrium state of within-host cells in an uninfected individual
209 in the absence of infection, X^* to be the equilibrium state of within-host cells in an
210 infected individual, and Y^* to be the equilibrium state of parasite density in an infected

211 individual, given by the expressions (derivations of which can be found in the electronic
 212 supplement):

$$213 \quad X' = \begin{cases} \frac{1 - \xi_1 Q}{\phi} & \text{if } 1 - \xi_2 Q > 0 \\ 0 & \text{otherwise} \end{cases} \quad (2a)$$

$$214 \quad X^* = \begin{cases} \frac{\gamma - \xi_2 Q \omega + \omega}{\epsilon} & \text{if } 1 - \xi_2 Q > 0 \\ \frac{\gamma}{\epsilon} & \text{if } 1 - \xi_2 Q \leq 0 \text{ \& } Y^* > 0 \\ X' & \text{if } 1 - \xi_2 Q \leq 0 \text{ \& } Y^* = 0 \end{cases} \quad (2b)$$

$$215 \quad Y^* = \begin{cases} \frac{\epsilon - \xi_1 Q \epsilon}{\gamma - \xi_2 Q \omega + \omega} - \phi & \text{if } 1 - \xi_2 Q > 0 \\ \frac{-\gamma \phi - \xi_1 \epsilon + \epsilon}{\gamma} & \text{if } 1 - \xi_2 Q \leq 0 \text{ \& } \frac{-\gamma \phi - \xi_1 \epsilon + \epsilon}{\gamma} > 0 \\ 0 & \text{if } \frac{-\gamma \phi - \xi_1 \epsilon + \epsilon}{\gamma} \leq 0 \end{cases} \quad (2c)$$

216

217 **Between-host model**

218 The dynamics of an infected population follow those of a simple susceptible - infected
 219 (S-I) model framework. Each individual can be classified into either healthy susceptible
 220 S or infected I and therefore the total population N is represented by $S + I$. We assume
 221 that new individuals enter the population at rate Λ . Transmission from a healthy
 222 susceptible individual to an infected individual occurs at rate θ proportional to the
 223 equilibrium status of within-host infection Y^* . We assume that the per capita mortality
 224 function u is the same for each class with rates $\frac{u}{1+kX'}$ and $\frac{u}{1+kX^*}$ for uninfected and
 225 infected individuals respectively, where k sets the strength of the mortality function
 226 with respect to the numbers of within-host cells. This ensures that cell depletion at the
 227 within-host level causes mortality at the level of the individual hosts, where the
 228 mortality function increases as the cell count decreases, up to a maximum value of u .

229 This also ensures that the death rate of an infected individual is inversely proportional
230 to the equilibrium state of the within-host cells under parasitisation.

231

232 The coupled within-host and population level model is a two-dimensional system of
233 non-linear ordinary differential equations (ODEs):

$$234 \quad \frac{dS}{dt} = \Lambda - \theta SIY^* - \frac{u}{1 + kX'} S \quad (3a)$$

$$235 \quad \frac{dI}{dt} = \theta SIY^* - \frac{u}{1 + kX^*} I \quad (3b)$$

236

237 The model was analysed using standard methods from dynamical systems theory and
238 were numerically solved with Wolfram Mathematica version number *10.0.2.0*. The
239 algebraic equilibria were found using the Mathematica function *Solve* and the numeric
240 equilibria by *NDSolve*. We ran simulations to determine parameter dependence of the
241 two systems of ODEs (which can be found in the electronic supplement). This analysis
242 shows that the between-host dynamics fall into sub-dynamics of the universal
243 behaviour of the model, regardless of parameter choice. For this reason, we chose a
244 set which highlights the typical qualitative behaviour and we examine how this
245 behaviour is modified by changing parameters around this standard set. The
246 parameter set we chose is one such set which highlights the qualitative behaviour of
247 the model, and which demonstrates the universal biological results obtained from the
248 model.

249

250 **Results**

251 **States of the population system, general case**

252 System (3) has two solutions; the endemic equilibria (EE) and the disease free
 253 equilibria (DFE).

$$254 \quad (S^{DFE}, I^{DFE}) = \left(\frac{\Lambda + k\Lambda X'}{u}, 0 \right) \quad (4a)$$

$$255 \quad (S^{EE}, I^{EE}) = \left(\frac{u}{\theta Y^* + k\theta X^* Y^*}, \frac{\Lambda + k\Lambda X^*}{u} - \frac{u}{\theta Y^* + k\theta X^* Y^*} \right) \quad (4b)$$

256 Therefore system (3) either converges to the EE or DFE depending upon the basic
 257 reproduction number R_0 , calculated as

$$258 \quad R_0 = \frac{\theta \Lambda Y^* (1 + kX') (1 + kX^*)}{u^2} \quad (5)$$

259 This tells us the threshold at which infection will spread throughout the population
 260 causing an epidemic ($R_0 > 1$). Increasing between-host transmission θ or population
 261 birth rate Λ increases the chance of outbreak. Increasing the density dependent
 262 mortality u decreases the chance of outbreak. The maximal value of R_0 here is
 263 maximised when the within-host functions Y^* , X^* and X' are maximised with respect
 264 to Q through the function $Y^*(1 + kX')(1 + kX^*)$. We predict that infection can spread
 265 through a population when the parasite load Y^* exceeds the critical threshold

$$266 \quad Y^* = \frac{u^2}{\theta \Lambda (1 + kX') (1 + kX^*)} \quad (6)$$

267 When the toxicant Q is not present in the system, we expect $R_0 = 1$ when $\phi \geq 0$, $\epsilon \geq$
 268 0 , $\gamma > 0$, $\omega \geq 0$, $\Lambda > 0$, $u > 0$, $\theta \geq 0$, $k \geq 0$ and

$$269 \quad 0 < \phi < \frac{\epsilon}{\gamma + \omega} \quad (7a)$$

$$270 \quad \theta + \frac{u^2 \epsilon \phi (\gamma + \omega)}{\Lambda (k + \phi) (\phi (\gamma + \omega) - \epsilon) (k (\gamma + \omega) + \epsilon)} = 0 \quad (7b)$$

271 When the toxicant is at a critical level where immunity is depleted at $Q = \frac{1}{\xi_2}$, we expect

272 $R_0 = 1$ when $\phi > 0$, $\epsilon > 0$, $\gamma \geq 0$, $\omega \geq 0$, $\Lambda > 0$, $u > 0$, $\theta \geq 0$, $k \geq 0$ and

273
$$0 < \xi_1 < \xi_2 \quad (8a)$$

274
$$0 < \gamma < \frac{\epsilon(\xi_2 - \xi_1)}{\xi_2\phi} \quad (8b)$$

275
$$\theta + \frac{\gamma\xi_2^2 u^2 \epsilon\phi}{\Lambda(\gamma k + \epsilon)(k(\xi_2 - \xi_1) + \xi_2\phi)(\gamma\xi_2\phi + \epsilon(\xi_1 - \xi_2))} = 0 \quad (8c)$$

276 When these conditions are met, the term $1 - \xi_2 Q$, is equal to 0, which corresponds to
 277 the point at which immunity is depleted $Z = 0$.

278

279 **Response to toxicant exposure, case of no infection**

280 Figure 2 shows the baseline dynamics of the model under the absence of within-host
 281 (and consequently between-host) infection. The lethality (reducing host function) of
 282 the toxicant linearly kills off the population of individuals in phase 0. Even though
 283 immune function is reduced, there is no parasite present to exploit and infect the
 284 population. After a threshold value all individual hosts are dead, and the population is
 285 extinct (phase V). This figure represents the baseline dynamics of the model under
 286 increasing toxicity and no infection.

287

288 **Response to toxicant exposure, case of sub-lethal effect dominating**
 289 **lethal effect**

290 Figure 3 shows the predicted stage of the epidemic under increasing toxicant exposure
 291 according to the simulations of the model. In general, there are 5 separate phases
 292 present in the model, as defined below (outbreak is denoted by *).

293

294 **Phase I: no population epidemic**

295 For low exposure to toxicant, the basic reproduction number is low ($R_0 < 1$). This
296 means that epidemics cannot occur at the population level. There is a very small
297 within-host infection burden (Y^*) which increases as the toxicant exposure increases.
298 In this phase, the individual parasite burden is not large enough to cause between-
299 host transmission and thus the population only declines a relatively small amount from
300 the direct exposure to the toxicant.

301

302 **Phase *II**: outbreak**

303 Here, the toxicant level is increased beyond a critical threshold causing $R_0 > 1$ and
304 outbreak at the population level. This threshold is determined by the relationship
305 between the within-host immunity, parasite burden and healthy cell status, and the
306 population rate of transmission (Eq. 5). This phase is characterised by a functioning
307 but declining immune status, caused by the increasing toxicant exposure. Combined
308 with a within-host parasite density reaching a peak at the end of phase *II**, we see an
309 outbreak of population level infection, and healthy susceptibles reaching a minimum,
310 while the total population decreases rapidly.

311

312 **Phase *III**: disease reduced**

313 Increasing the toxicant exposure further results in a complete depletion of the within-
314 host immune status. The basic reproduction number of the infection begins to drop
315 resulting in fewer infected cases and therefore an increase in healthy individuals.
316 Infected individuals are killed off by the mortality induced by the epidemic. This higher
317 level of toxicant exposure causes the parasite density to drop below the minimum
318 required for an infection to spread at the population level (determined by Eq. 6). This

319 means that the total population is able to recover marginally due to the infection being
320 removed.

321

322 **Phase IV: disease controlled**

323 At the start of phase IV, the population epidemic is over ($R_0 < 1$). As the toxicant
324 exposure is increased again, the within-host parasite density decreases to 0. At these
325 very high levels of exposure, the individuals are killed by the direct mortality inducing
326 toxicant causing the population to decline once again.

327

328 **Phase V: host dead**

329 At extremely high levels of exposure the host is killed due to the lethality of the toxicant.
330 All within-host functions are depleted. This results in the population reaching
331 extinction.

332

333 **Response to toxicant exposure, case of lethal effect dominating sub-** 334 **lethal effect and case of no lethal effect**

335 We explore the case of the absence of toxicant exposure ($\xi_1 = 0$) in Fig. ES1, and
336 also the case of aggressive toxicant exposure (ξ_1 larger than ξ_2) in Fig. ES2. Both of
337 these figures can be found in the electronic supplementary information.

338

339 Setting the lethal toxicant exposure $\xi_1 = 0$ (Fig. ES1) results in similar phase based
340 dynamics observed in Fig. 3. Under this condition, the first stages of the epidemic can
341 be divided into phases I and II*, qualitatively identical to those found in Fig. 3.
342 However, after the host immune function is destroyed, a new phase III*b occurs for
343 any increasing value of toxicant. This results in a persistent epidemic caused by the

344 lack of any lethal effects of the toxicant. In this case, the basic reproduction number
345 remains constant for all further toxicant exposure. Therefore, the low toxicant
346 behaviour of the model is similar to the original, even after removing this lethal toxicant
347 effect $\xi_1 = 0$.

348

349 We set the lethal toxicant effect higher than the sublethal effect in Fig. ES2. This is in
350 order to examine the effect of reversing the assumption used throughout this paper
351 ($\xi_2 < \xi_1$). We see that this alternative assumption predicts three phases of the
352 epidemic which are broadly similar to those found in Fig. 3. The individual is highly
353 infective to begin with and then the lethal toxicant effect begins to remove the within-
354 host parasite density. After this, the population level infection is removed from the
355 system, and the model returns back to phases *IV* and *V* seen in the original dynamical
356 behaviour of the model.

357

358 Both of these figures highlight similar epidemiological phases of the model under
359 different assumptions and are sub-dynamics of the original dynamics found in Fig. 3.

360

361 **Within-host parameter phase dependence**

362 Here, we outline the behaviour of the model for a wider range of pairwise parameters.
363 We do this in order to investigate the effects of slight changes to our original parameter
364 set, and to see how the trade-offs between important within- and between-host
365 functions determine the subsequent population epidemic. We define the phases as
366 above, with phase 0 representing the region where there is no feasible within-host or
367 between-host disease.

368

369 **Direct lethal effect ξ_1 and sublethal ξ_2 toxicant effect**

370 Figure 4 shows the predicted phase of the population epidemic for 3 different levels of
371 toxicant exposure, and for a range of lethal toxicant effect (relative to the production
372 of new within-host cells) and sublethal toxicant effect (relative to the production of
373 immunity). The white regions in Fig. 4 show the space in which the assumption ($\xi_2 <$
374 ξ_1) is broken. First, the absence of toxicant exposure ($Q = 0$) results in no such
375 epidemic for any value of lethal and sublethal toxicant effect. Second, as the toxicant
376 exposure is increased to an intermediate value ($Q = 0.50$), outbreak (phase II^*) occurs
377 when the toxicant has both sufficiently high lethal and high sublethal effect. Third, as
378 the toxicant reaches high levels ($Q = 1.50$), the outcome of the outbreak can fall into
379 any of the phases of epidemiology ($0 - V$), dependent upon the respective lethal and
380 sublethal properties of the toxicant. Higher lethal and sublethal toxicant stress can
381 result in the extinction of the population, whereas lower lethality and higher sublethal
382 effects are required for outbreak (phases II^* and III^*).

383

384 **Within-host transmission and production of cells (relative to removal of**
385 **immunity) ϵ and between-host transmission θ .**

386 Figure 5 likewise shows the predicted phase for a range of different levels of ϵ and θ .
387 In the absence of toxicant ($Q = 0$), outbreak can only occur (II^*) if the within-host
388 transmission and production of cells ϵ is sufficiently high. Otherwise, no epidemic can
389 occur for any value of between-host transmission. Secondly as the toxicant is
390 increased to an intermediate value ($Q = 1.00$), the epidemic occurs (III^*) if both
391 parameters are sufficiently large. Third, at extremely high levels of exposure ($Q =$
392 2.00), the population becomes extinct.

393

394 **Birth rate Λ and mortality rate u**

395 Figure 6 shows the relationship between the between-host birth and death rates and
396 the predicted stage of the epidemic. In the absence of toxicant exposure ($Q = 0$), there
397 are 2 possible outcomes. A low death rate is required to see the outbreak of the
398 disease. Otherwise between-host disease is not possible for any choice of Λ and u .
399 Increasing the toxicant exposure to higher levels ($Q = 1.00$) results in a complete
400 switch to either the reduction or control of the disease. Finally, increasing the exposure
401 to an extremely high level ($Q = 2.00$) results in host death and the extinction of the
402 population.

403

404 **Discussion**

405 We have studied and analysed a nested multi-level model of within and between-host
406 processes to understand how toxicants impact epidemiological dynamics. A key
407 finding is that population epidemics are dependent upon the level of toxicant exposure.
408 In general, infection prevalence is maximised by intermediate levels of toxicant. We
409 classify this population epidemic into 5 phases showing that any outbreak is
410 dependent on the toxicant's sublethal and lethal properties. Higher toxicant exposure
411 results in either outbreak of infection or death of the population. In particular, the
412 stress-mediated within-host statuses of immune function and parasite load also
413 determine the outcome of the epidemic at the population level.

414

415 Importantly our model predicts that epidemics may not occur until reaching an
416 intermediate threshold exposure of toxicant. At low levels of exposure, the parasite
417 density is able to increase but between-host infection is equal to zero within the
418 population until reaching a critical threshold (at the start of phase II^*). Sub-lethal

419 toxicant exposure can have dramatic consequences for population epidemiology,
420 causing widespread outbreak. These results support the body of work on synergistic
421 interactions between environmental chemicals and natural stressors (Holmstrup et al.
422 2010), and highlight the effects of toxicants on higher scales of organisation such as
423 population dynamics, which are often not understood (Kohler and Triebkorn 2013) or
424 difficult to experimentally test (Gergs et al. 2013).

425

426 Our model also predicts that population epidemics follow phase-based transitions
427 dependent on the level of toxicant exposure. Within our model, 5 such phases are
428 present. First, the parasite burden is too small within individuals to have any impact
429 on the population level. Only when the parasite density crosses a minimum threshold
430 (Eq. 6) do we see any population level impact. The immunosuppressive toxicant effect
431 causes the parasite density to rapidly multiply and spread between individuals. Under
432 increasing exposure, prevalence only subsides when the parasite is reduced by the
433 lethal toxicant effect. The sublethal immunosuppressive effect of the toxicant only
434 impacts the population if the toxicant exposure is low. Otherwise the lethality of the
435 toxicant takes over and kills the host, causing extinction of the population. These
436 complicated phase-based epidemics show that the effect of toxicant exposure upon
437 population disease outbreak is non-linear. Interestingly, when considering the
438 population density under increasing toxicant exposure we see a rapid decrease in the
439 population in the early and late stages of this exposure. However, in phase *III**, we
440 see a marginal increase in the density which represents population recovery. This is
441 caused by a significant reduction in the epidemiological dynamics and means that the
442 healthy population is able to recover. This has implications for environmental
443 assessors, where often the indicator of an ecosystem's healthy state is population

444 density, rather than the individual clinical states of a system. Our results suggest that
445 by only monitoring population density the underlying dynamics may go unnoticed,
446 especially in the predicted mid-range toxicant phase *III**.

447

448 A further prediction the model makes is that trade-offs between within- and between-
449 host functions determine the subsequent population epidemiology (Fig. 4, Fig. 5 and
450 Fig. 6). We show that outbreak will occur when the individual sublethal toxicant effect
451 is relatively higher than that of the lethal effect. Although we also predict that higher
452 exposure to toxicants can result in any of the defined epidemiological phases. This
453 suggests that population epidemiology can be completely determined by the relative
454 sublethal and lethal properties of the toxicant. In addition, we also show that the
455 sublethal toxicant effect determines whether the population will become extinct at high
456 toxicant exposure. This further suggests that the individual properties of toxicants are
457 important in determining outbreak. The trade-off between different scales of
458 transmission also determine these phase-based epidemics. In general, higher levels
459 of both within- and between-host transmission result in outbreak. Another implication
460 of these phase-based plots are that slight increases in parameters can result in sudden
461 epidemiological switches. For example, the third panel in Fig. 4 shows all of the phases
462 in our system. A slight increase in the sublethal effect ξ_2 at this high toxicant exposure
463 $Q = 1.50$ can result in abrupt transitions between phase 0 or *I* to phase *IV*. These kind
464 of transitions show that these phases of epidemiology are sensitive to slight
465 perturbations in the effects of sublethal and lethal toxicant exposure. Introducing a
466 new toxicant into a healthy population with only a slightly stronger sublethal effect on
467 the host could cause a dramatic regime shift and ultimately high mortality rates (shift
468 from phase *I* to phase *IV*).

469

470 The results in the main text of this paper depend entirely upon the relative sublethal
471 and lethal effects of the toxicant, particularly on the assumption that $\xi_2 > \xi_1$. We
472 focussed on this assumption for multiple reasons. If this assumption were reversed,
473 the within-host model predicts unrealistically that the immune function will be present
474 even after the host is dead. In Fig. ES2 we show that under this reverse assumption,
475 the results still fall into the phase-based transitions seen under the normal assumption
476 and are sub-dynamics of the original phases shown in Fig 3. Another reason we focus
477 on the case of $\xi_2 > \xi_1$ is because direct chronic lethality often occurs at higher doses
478 of toxicant (Suchail et al. 2001, Pan et al. 2014, Wang et al. 2017) and
479 immunosuppressive damage occurs at various levels of lower dose toxicant exposure
480 (Bols et al. 2001, James and Xu 2012, Brandt et al. 2016). Therefore, we argue that
481 focussing on the case in which host mortality occurs at higher toxicant exposure and
482 immunosuppressive damage occurs at lower, sublethal levels is biologically realistic.

483

484 A previous study, Booton et al. (2018) used a simple modelling framework to describe
485 the within-host infection dynamics under toxicant exposure in an individual. This work
486 demonstrated that an intermediate exposure of toxicant maximised within-host
487 parasite density. In this paper, we introduced a nested modelling framework based on
488 the within-host model used in Booton et al. (2018), which extends the previous model
489 to the epidemiological between-host population level. We did this in order to examine
490 how epidemiological parameters interact with within-host processes, showing that
491 population epidemics are determined by the level of toxicant exposure, which can be
492 divided into 5 such phases. Few studies examine the interaction between toxicant
493 stress and within-host processes, and even fewer then relate this to the population

494 scale (Lundin et al. 2015, Bhattacharya and Martcheva 2016). The novelty therefore
495 in this paper is the consideration of both within- and between-host scales, as opposed
496 to the singular scale examined in Booton et al. (2018). By relating these scales with
497 toxicant exposure, we were able to classify the complicated relationship between
498 increasing toxicant exposure and the spread of disease at the population level. We
499 show how R_0 changes with respect to between-host parameters, showing that an
500 increase in between-host transmission or birth rate, a decrease in mortality, or an
501 increase in the relative effect of host mortality (Fig. ES3) increases the chance of
502 outbreak. In addition, the maximal value of R_0 is determined by the trade-off between
503 the within-host functions, as shown in Eq. (5). This maximal value is equivalent to the
504 point at which the within-host cells in infected individuals level out and where the
505 within-host parasite density is maximised, for all parameters. Therefore, the value of
506 Q which maximises the within-host parasite density is equal to the value which
507 maximises the spread of infection at the population level. This is an interesting result,
508 and can be explained through the identical 'turning point' found for all within-host
509 processes (as demonstrated for example in Fig. 3, at $Q = 0.5$). This results from the
510 depletion of the immune system, whereby the total population level risk of infection is
511 maximised when those individuals within the population have weakened immune
512 responses as a result of sublethal toxicant exposure.

513

514 These results have a number of applications, one such application being motivated by
515 the impacts that toxicants have on a wide range non-target species (Phipps and
516 Holcombe 1985, Snell and Janssen 1995, Van Den Berg et al. 1998, Eason et al.
517 2002, Buratini et al. 2004, Relyea and Hoverman 2006, Goulson et al. 2015, Pisa et
518 al. 2015). For example, the recent and widespread losses in worldwide bee

519 populations (Goulson et al. 2015) are thought to be caused by multifactorial synergistic
520 stressors (Alaux et al. 2010, Neumann and Carreck 2010, Potts et al. 2010, Ratnieks
521 and Carreck 2010, Vanbergen 2013). Within this setting, this work fills a previously
522 identified research gap (Lundin et al. 2015) by outlining the complicated relationship
523 between toxicant stress and population epidemics. In general, increased exposure to
524 toxicants should result in more colony epidemics and therefore greater population
525 losses. Intermediate exposure to toxicants could result in dramatic decreases in
526 overall colony health. Reducing the sublethal toxicant exposure below the predicted
527 safe phase *I* threshold (to ensure $R_0 < 1$ in Eq. 5) ensures that no colony epidemic
528 can occur. These results highlight the nonlinear relationship between pesticide
529 exposure and population epidemiology. Indeed, the very general nature of this model
530 means that these results may be applied to any enviro-epidemiological system
531 exposed to disease.

532

533 The framework presented in this study focusses on linking two scales of biological
534 organisation under toxicant stress. This toxicant stress affects the within-host
535 dynamics in two ways, acting as an indirect immunosuppressant and directly
536 impacting the vital functionality of individual health. A further improvement to the model
537 could investigate the role of social immunity, a process by which populations prevent
538 infection from spreading. Social insects are known to perform behavioural traits such
539 as removing diseased or dead individuals (Spivak and Gilliam 1998), preventing
540 others from interacting with infected individuals (Waddington and Rothenbuhler 1976),
541 and collectively raising the temperature of the surrounding environment through a
542 process known as social fever (Starks et al. 2000), all in order to prevent further
543 infection. Incorporating these social mechanisms into our nested multilevel modelling

544 framework could shed new light on the way that populations use innate and social
545 immunity to combat disease.

546

547 In summary, this work takes a multifactorial approach to model infection at the
548 population level which can be divided into 5 phases dependent upon the level of
549 toxicant stress. We predict that infection within populations is maximised by
550 intermediate toxicant exposure, and that there exists a toxicant threshold below which
551 individual parasite density is controlled and outbreak does not occur. The modelling
552 framework used here presents a starting position to think about how within-host
553 functions such as immunity and parasite density determine population level effects.
554 This work highlights the need for experimental studies which focus on measuring
555 epidemiological traits of populations under increasing toxicant exposure.

556

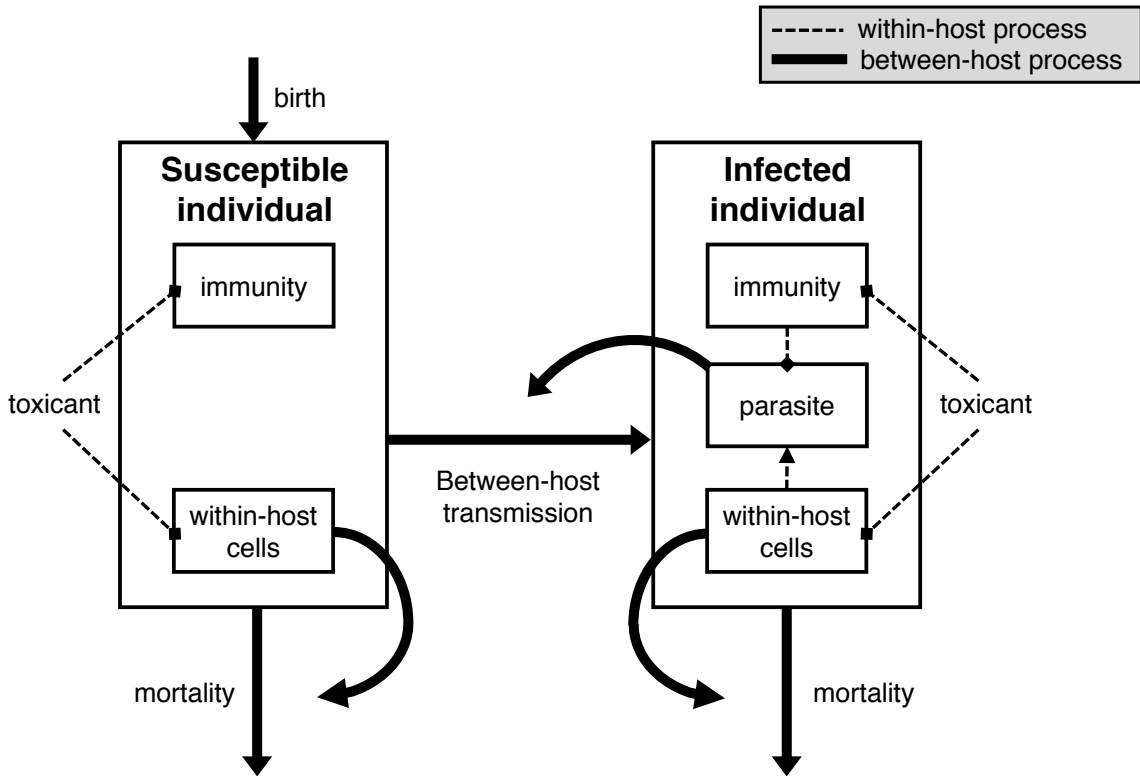
557 **Declarations**

558 This work was supported by a Japan Society for the Promotion of Science (JSPS)
559 BRIDGE Fellowship and a University of Sheffield PhD scholarship to R.D.B. All
560 authors conceived the idea for the study, constructed the model and analysed and
561 interpreted the material. We would like to thank two anonymous reviewers and Dr.
562 Francois Massol for their constructive comments which improved this manuscript.
563 R.D.B. wrote the manuscript, with contributions from all authors.

564 We declare we have no competing interests.

565

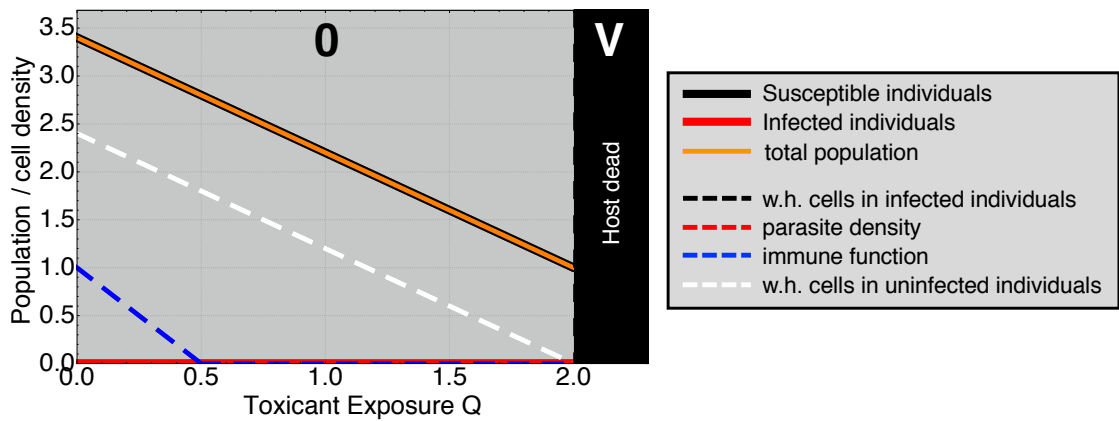
566 **Figures and tables**



567

568 *Figure 1: The outline of the multilevel model. Bold lines show the between-host processes and dashed show the*
 569 *within-host processes. Individuals can either be classified as susceptible or infected. Infection spreads between*
 570 *hosts dependent upon the within-host parasite density. The toxicant impacts immune function and the general*
 571 *functionality of the host. New individuals enter the system via birth and leave via death which is dependent upon*
 572 *the individual within-host cellular health status.*

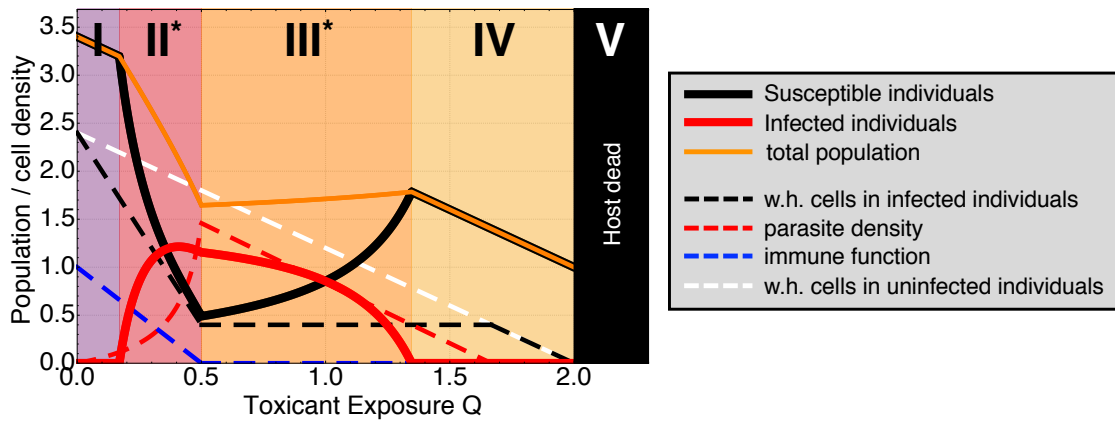
573



574

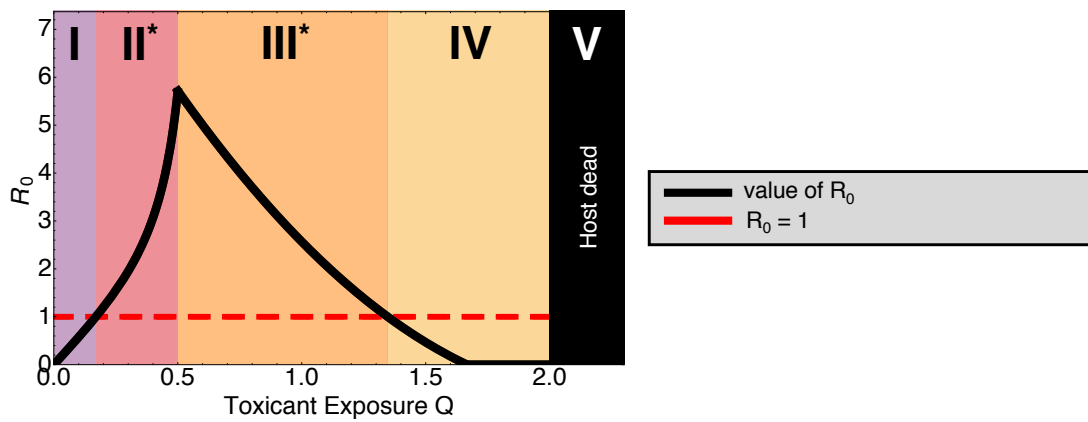
575 *Figure 2: The baseline dynamics of the model without initial within-host infection. The absence of the within-host*
 576 *infection means that the infection cannot spread to the population level. Phase 0 corresponds to the region of no*
 577 *feasible infection and phase V corresponds to the death of all individuals within the population. Parameters as in*
 578 *Table 1, but with the initial parasite density $Y^* = 0$.*

579



580

581 (a)

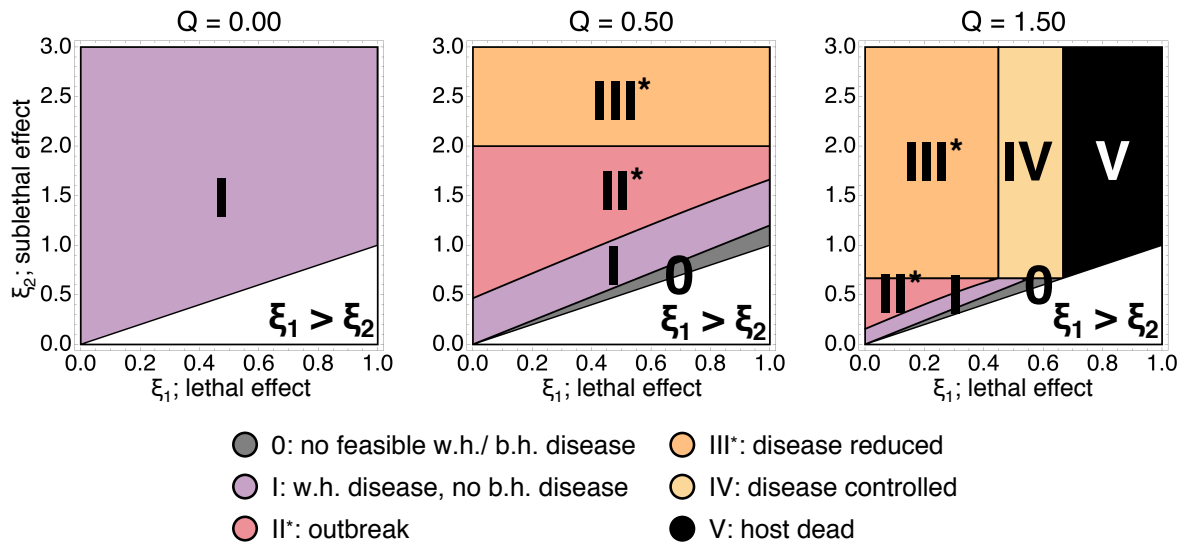


582

583 (b)

584 *Figure 3: The predicted five phases of an infected population under increasing toxicant stress Q . Starred phases*
 585 *(II* and III*) represent the outbreak of infection where $R_0 > 1$. In (a) solid lines represent the population dynamics*
 586 *and dashed lines the within-host dynamics. In (b) the black line shows the value of R_0 and the dashed red line*
 587 *shows the threshold at which $R_0 = 1$ and above which outbreak will occur within the population. Parameters taken*
 588 *from Table 1.*

589

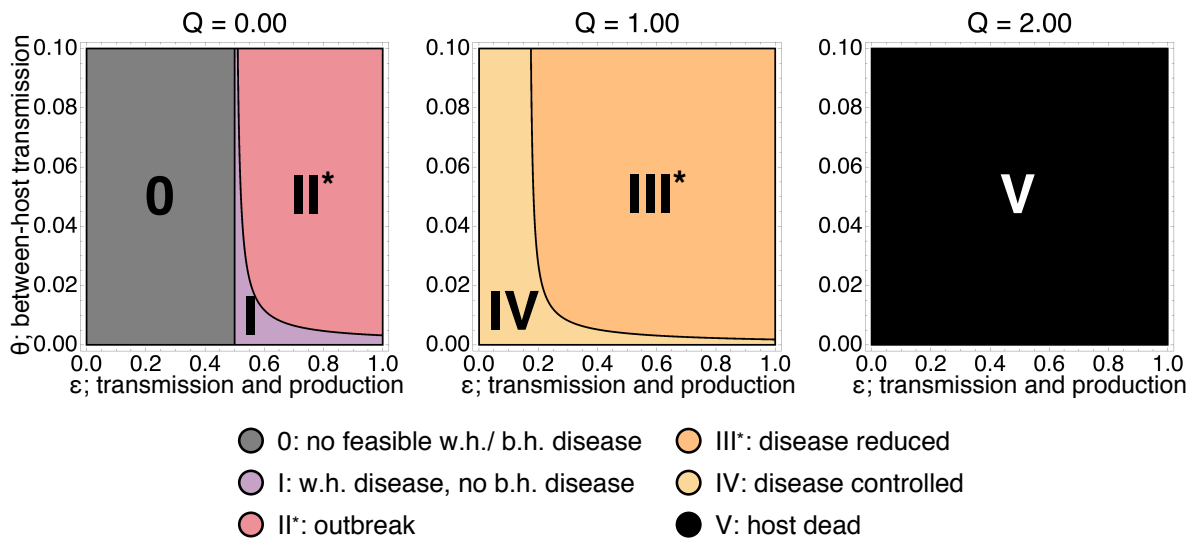


590

591 *Figure 4: The predicted phase (0 – V) epidemiological outcome of the population level dynamics for 3 levels of*
 592 *toxicant exposure and varying direct lethal toxicant effect (relative to the production of new within-host cells) ξ_1 and*
 593 *sublethal effect (relative to the production of immunity) ξ_2 . Note that the white region represents the phase space*
 594 *under which the assumption $\xi_2 > \xi_1$ is no longer valid. Starred phases (II* and III*) represent the outbreak of*
 595 *infection within the population. For the absence of toxicant exposure $Q = 0$, outbreak cannot occur for any value*
 596 *of ξ_1 and ξ_2 . For intermediate $Q = 0.50$, outbreak occurs if the values of ξ_1 and ξ_2 are sufficiently large. For lethal*
 597 *$Q = 1.50$, any of the phases can occur dependent upon the choice of ξ_1 and ξ_2 . High values of ξ_1 and ξ_2 result in*
 598 *extinction of the population. Parameters as in Table 1, but for varying ξ_1 and ξ_2 as above.*

599

600



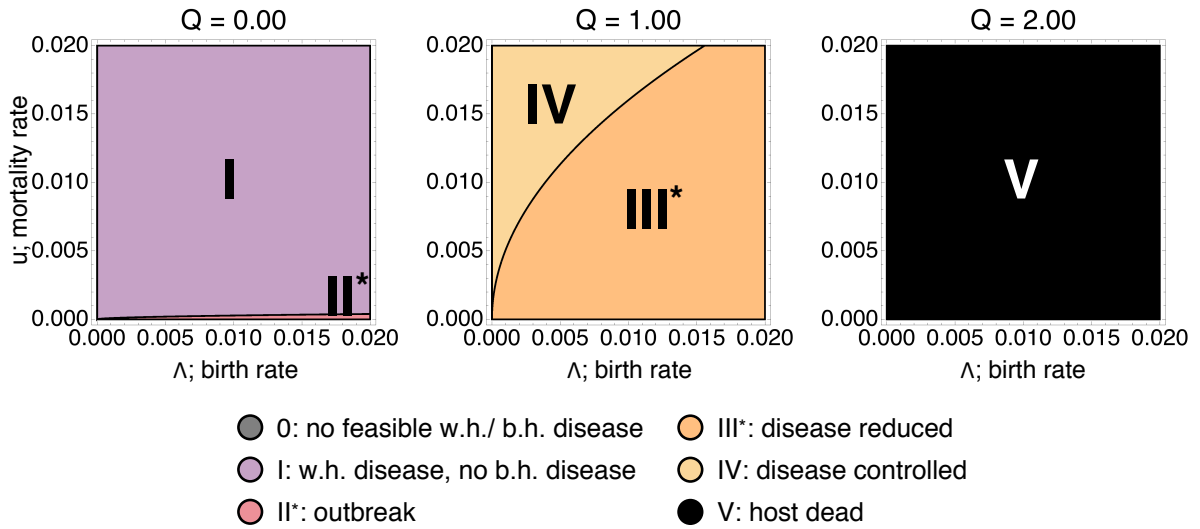
601

602 *Figure 5: The dynamical phase (0 – V) for a range of within-host transmission and production of cells (relative to*
 603 *the removal of immunity) ϵ and between-host transmission θ . Starred phases (II* and III*) represent the*
 604 *outbreak of infection within the population. For $Q = 0$, outbreak will occur (II*) if ϵ is sufficiently large, otherwise*
 605 *phase 0 will occur for any value of θ . For $Q = 1.00$, phase III* occurs only if both ϵ and θ are large enough. For*
 606 *high $Q = 2.00$, population extinction occurs for any chosen values of ϵ and θ . Parameters as in Table 1, but for*
 607 *varying ϵ and θ .*

608

609

610



611
 612
 613
 614
 615
 616
 617

Figure 6: The predicted phase (0 – V) for a range of between-host birth rate Λ and between-host mortality u . Starred phases (II* and III*) represent the outbreak of infection within the population. For $Q = 0$, outbreak will occur (II*) if u is sufficiently low. For $Q = 1.00$, either outbreak III* occurs or phase IV occurs depending on the choice of Λ and u . For $Q = 2.00$, all hosts are dead and extinction of the population occurs. Parameters as in Table 1, but for varying transmission parameters Λ and u .

<i>Parameter/ variable description</i>	<i>Symbol</i>	<i>Value</i>	<i>Units</i>
Within-host			
Within-host uninfected cells	X		No dimension
Parasite density	Y		No dimension
Immune function	Z		No dimension
Lethal toxicant effect relative to production of new cells	ξ_1	0.5	No dimension
Sublethal toxicant effect relative to production of immunity	ξ_2	2	No dimension
Mortality of cells relative to removal of immunity	ϕ	0.4166	No dimension
Mortality of parasite relative to removal of immunity	γ	0.2	No dimension
Within-host transmission and production of cells relative to removal of immunity	ϵ	0.5	No dimension
Suppression and production of immunity relative to removal of immunity	ω	1	No dimension
Between-host			
Susceptible individuals	S		Individuals
Infected individuals	I		Individuals
Birth rate	Λ	0.01	Individuals time ⁻¹
Between-host transmission rate	θ	0.01	Individuals ⁻¹ time ⁻¹
Mortality rate	u	0.01	Time ⁻¹
Relative effect of host mortality	k	1	No dimension

618

619 *Table 1: The between and within-host parameters used in the analysis and simulations of the model, and their respective*
620 *units. For the within-host parameters and their units used in Booton et al. 2018, please see the electronic supplementary*
621 *information.*

622

623 **References**

624 Alaux, C. et al. 2010. Interactions between *Nosema* microspores and a neonicotinoid
625 weaken honeybees (*Apis mellifera*). – *Environ. Microbiol.* 12: 774–782.

626

627 Alizon, S. and van Baalen, M. 2005. Emergence of a convex trade-off between
628 transmission and virulence. – *Am. Nat.* 165: E155–E167.

629

630 Anderson, R. and May, R. 1992. Infectious diseases of humans: dynamics and
631 control. – Oxford University Press, Oxford.

632

633 Bhattacharya, S. and Martcheva, M. 2016. An immuno-eco-epidemiological model of
634 competition. – *J. Biol. Dyn.* 10: 314–341.
635

636 Blacquièrè, T. et al. 2012. Neonicotinoids in bees: a review on concentrations, side-
637 effects and risk assessment. – *Ecotoxicology* 21: 973–992.
638

639 Bols, N. C. et al. 2001. Ecotoxicology and innate immunity in fish. – *Dev. Comp.*
640 *Immunol.* 25: 853–873.
641

642 Booton, R. et al. 2017. Stress-mediated Allee effects can cause the sudden collapse
643 of honey bee colonies. – *J. Theor. Biol.* 420: 213–219.
644

645 Booton, R. et al. 2018. Interactions between immunotoxicants and parasite stress:
646 implications for host health. – *J. Theor. Biol.* 445: 120–127.
647

648 Brandt, A. et al. 2016. The neonicotinoids thiacloprid, imidacloprid, and clothianidin
649 affect the immunocompetence of honey bees (*Apis mellifera* L.). – *J. Insect Physiol.*
650 86: 40–47.
651

652 Bryden, J. et al. 2013. Chronic sublethal stress causes bee colony failure. – *Ecol.*
653 *Lett.* 16: 1463–1469.
654

655 Buratini, S. et al. 2004. Evaluation of *Daphnia similis* as a test species in
656 ecotoxicological assays. – *Bull. Environ. Contam. Toxicol.* 73: 878–882.
657

658 Coors, A. et al. 2008. Pesticide exposure strongly enhances parasite virulence in an
659 invertebrate host model. – *Oikos* 117: 1840–1846.
660

661 Davies, P. et al. 1994. Sublethal responses to pesticides of several species of
662 Australian freshwater fish and crustaceans and rainbow trout. – *Environ. Toxicol.* 570
663 *Chem.* 13: 1341–1354.
664

665 Decourtye, A. et al. 2003. Learning performances of honeybees (*Apis mellifera* L.)
666 are differentially affected by imidacloprid according to the season. – *Pest Manag.*
667 *Sci.* 59: 269–278.
668

669 Doublet, V. et al. 2015. Bees under stress: sublethal doses of a neonicotinoid
670 pesticide and pathogens interact to elevate honey bee mortality across the life cycle.
671 – *Environ. Microbiol.* 17: 969–983.
672

673 Eason, C. et al. 2002. Assessment of risks of brodifacoum to non-target birds and
674 mammals in New Zealand. – *Ecotoxicology* 11: 35–48.
675

676 Feng, Z. et al. 2015. Coupled within-host and between-host dynamics and evolution
677 of virulence. – *Math. Biosci.* 270: 204–212.
678

679 Feng, Z. et al. 2013. A mathematical model for coupling within-host and between
680 host dynamics in an environmentally-driven infectious disease. – *Math. Biosci.* 241:
681 49–55.
682

683 Feng, Z. et al. 2012. A model for coupling within-host and between-host dynamics in
684 an infectious disease. – *Nonlinear Dyn.* 68: 401–411.
685

686 Gergs, A. et al. 2013. Chemical and natural stressors combined: from cryptic effects
687 to population extinction. – *Sci. Rep.* 3: 2036.
688

689 Gilbertson, M. et al. 2003. Immunosuppression in the northern leopard frog (*Rana*
690 *pipiens*) induced by pesticide exposure. – *Environ. Toxicol. Chem.* 22: 101–10.
691

692 Gilchrist, M. and Coombs, D. 2006. Evolution of virulence: Interdependence,
693 constraints, and selection using nested models. – *Theor. Popul. Biol.* 69: 145–153.
694

695 Gilchrist, M. and Sasaki, A. 2002. Modeling host-parasite coevolution: a nested
696 approach based on mechanistic models. – *J. Theor. Biol.* 218: 289-308.
697

698 Gill, R. et al. 2012. Combined pesticide exposure severely affects individual-and
699 colony-level traits in bees. – *Nature* 491: 105–108.
700

701 Goulson, D. et al. 2015. Bee declines driven by combined stress from parasites,
702 pesticides, and lack of flowers. – *Science* 347: 1255957.
703

704 Grenfell, B. and Harwood, J. 1997. (Meta)population dynamics of infectious
705 diseases. – *Trends Ecol. Evol.* 12(10): 395–399.
706

707 Han, P. et al. 2010. Quantification of toxins in a Cry1Ac + CpTI cotton cultivar and its
708 potential effects on the honey bee *Apis mellifera* L. – *Ecotoxicology* 19:1452–1459.
709

710 Henry, M. et al. 2012. A common pesticide decreases foraging success and survival
711 in honey bees. – *Science* 336: 348–350.
712

713 Heugens, E. et al. 2006. Population growth of *Daphnia magna* under multiple stress
714 conditions: joint effects of temperature, food, and cadmium. – *Environ. Toxicol.*
715 *Chem.* 25: 1399–1407.
716

717 Holmstrup, M. et al. 2010. Interactions between effects of environmental chemicals
718 and natural stressors: a review. – *Sci. Total Environ.* 408: 3746–3762.
719

720 Iwasa, T. et al. 2004. Mechanism for the differential toxicity of neonicotinoid
721 insecticides in the honey bee, *Apis mellifera*. – *Crop Prot.* 23: 371–378.
722

723 James, R. R. and Xu, J. 2012. Mechanisms by which pesticides affect insect
724 immunity. – *J. Invertebr. Pathol.* 109: 175–182.
725

726 Kohler, H. and Triebkorn, R. 2013. Wildlife ecotoxicology of pesticides: Can we
727 track effects to the population level and beyond? – *Science* 341: 759–765.
728

729 Lundin, O. et al. 2015. Neonicotinoid insecticides and their impacts on bees: a
730 systematic review of research approaches and identification of knowledge gaps. –
731 *PLoS ONE* 10: e0136928.

732

733 Martin, T. and Holdich, D. 1986. The acute lethal toxicity of heavy metals to
734 peracarid crustaceans (with particular reference to fresh-water asellids and
735 gammarids). – *Water Res.* 20: 1137–1147.

736

737 Mason, R. 2013. Immune suppression by neonicotinoid insecticides at the root of
738 global wildlife declines. – *J. Environ. Immunol. Toxicol.* 1: 3–12.

739

740 Mideo, N. et al. 2008. Linking within- and between-host dynamics in the evolutionary
741 epidemiology of infectious diseases. – *Trends Ecol. Evol.* 23: 511–517.

742

743 Neumann, P. and Carreck, N. 2010. Honey bee colony losses. – *J. Apic. Res.* 49: 1–
744 6.

745

746 Nowak, M. and May, R. 2000. *Virus dynamics: mathematical principles of*
747 *immunology and virology: mathematical principles of immunology and virology.* –
748 Oxford Univ. Press.

749

750 Pan, H. et al. 2014. Lethal and sublethal effects of cycloxaprid, a novel cis-
751 nitromethylene neonicotinoid insecticide, on the mirid bug *Apolygus lucorum*. – *J.*
752 *Pest. Sci.* 87: 731–738.

753

754 Pettis, J. et al. 2012. Pesticide exposure in honey bees results in increased levels of
755 the gut pathogen *Nosema*. – *Naturwissenschaften* 99: 153–158.

756

757 Phipps, G. and Holcombe, G. 1985. A method for aquatic multiple species toxicant
758 testing: acute toxicity of 10 chemicals to 5 vertebrates and 2 invertebrates. –
759 Environ. Pollut. A 38: 141–157.
760

761 Pisa, L. et al. 2015. Effects of neonicotinoids and fipronil on non-target invertebrates.
762 – Environ. Sci. Pollut. Res. 22: 68–102.
763

764 Potts, S. et al. 2010. Global pollinator declines: trends, impacts and drivers. – Trends
765 Ecol. Evol. 25: 345–353.
766

767 Ratnieks, F. and Carreck, N. 2010. Clarity on honey bee collapse? – Science 327:
768 645 152–153.
769

770 Relyea, R. and Hoverman, J. 2006. Assessing the ecology in ecotoxicology: a review
771 and synthesis in freshwater systems. – Ecol. Lett. 9: 1157–1171.
772

773 Snell, T. and Janssen, C. 1995. Rotifers in ecotoxicology: a review. – Hydrobiologia
774 313-314: 231–247.
775

776 Spivak, M. and Gilliam, M. 1998. Hygienic behaviour of honey bees and its
777 application for control of brood diseases and Varroa. Part II. Studies on hygienic
778 behaviour since the Rothenbuhler era. – Bee World 79: 169–186.
779

780 Starks, P. et al. 2000. Fever in honeybee colonies. – Naturwissenschaften 87: 229–
781 231.

782

783 Suchail, S. et al. 2001. Discrepancy between acute and chronic toxicity induced by
784 imidacloprid and its metabolites in *Apis mellifera*. – *Environ. Toxicol. Chem.* 20:
785 2482–2486.

786

787 Van Den Berg, M. et al. 1998. Toxic equivalency factors (TEFs) for PCBs, PCDDs,
788 PCDFs for humans and wildlife. – *Environ. Health Perspect.* 106: 775–792.

789

790 Vanbergen, A. 2013. Threats to an ecosystem service: pressures on pollinators. –
791 *Front. Ecol. Environ.* 11: 251–259.

792

793 Vidau, C. et al. 2011. Exposure to sublethal doses of fipronil and thiacloprid highly
794 increases mortality of honeybees previously infected by *nosema ceranae*. – *PLoS*
795 *ONE* 6: e21550.

796

797 Waddington, K. and Rothenbuhler, W. 1976. Behaviour associated with hairless
798 black syndrome of adult honeybees. – *J. Apic. Res.* 15: 35–41.

799

800 Wang, R. et al. 2017. Lethal and sublethal effects of cyantraniliprole, a new
801 anthranilic diamide insecticide, on *Bemisia tabaci* (Hemiptera: Aleyrodidae) MED. –
802 *Crop Prot.* 91: 108–113.

803

804 Warner, R. et al. 1966. Behavioural pathology in fish: a quantitative study of
805 sublethal pesticide toxication. – *J. Appl. Ecol.* 3: 223–247.

806

807 Williams, G. R. et al. 2015. Neonicotinoid pesticides severely affect honey bee
808 queens. – Sci. Rep. 5: 14621.

809

810 Williamson, S. and Wright, G. 2013. Exposure to multiple cholinergic pesticides
811 impairs olfactory learning and memory in honeybees. – J. Exp. Biol. 216: 1799–
812 1807.